Monte Carlo Investigation of Potential Fluctuation in 3D Device Structure

Y. Ohkura and C. Suzuki, N. Mise, T. Matsuki, T. Eimori, and M. Nakamura
Semiconductor Leading Edge Technologies, Inc.
Tsukuba, JAPAN

***Abstract*—The motions of particles are calculated in 3D structure to evaluate potential fluctuation. The results of homogeneous and thermal equilibrium systems are in good agreement with theoretical results. In 3D MOSFET, the potential fluctuation extends towards the depletion layer and deviation of the amplitude from theoretical value is observed and ascribed to hot electron energy distribution, so the conventional plasmon scattering model should be modified in non-uniform and non-equilibrium carrier distribution.**

Keywords-component; potential fluctuation, Monte Carlo, nonequilibrium, inhomogeneou

I. INTRODUCTION

In the semiconductor, electric field continuously changes by Coulomb interaction due to the motion of electrons. But in the case of 2D analysis, each carrier corresponds to a line charge, so the Coulomb force is unnatural even if plasmon and carrier-carrier scattering model [1][2] is included. In Ref. [2], 2D simulation could mimic satisfactorily the correct behavior of 3D systems. But the distribution of plasmon is assumed to be in thermal-equilibrium. Tsuchiya et al. [3] pointed out that if the temperature of plasmon model is assumed to be the lattice temperature, the electron energy is excessively relaxed down to the thermal energy, so, they used the electron temperature to evaluate the plasmon scattering rates. However, in non-equilibrium state, the definition of the electron temperature is thought to be an issue to investigate.

On the other hand, the plasma oscillations were explicitly demonstrated through 3D MC simulation recently [4]. Nevertheless, any comparative study on the amplitude of potential oscillation has not been reported in 3D simulation.

Thus in this study, firstly the potential fluctuation and its relation to plasmon is investigated for homogeneous structure in thermal-equilibrium state, and then the potential fluctuation (standard deviation) in non-equilibrium transport of 3D MOSFET is investigated using in-house simulator HyDeLEOSMC [5].

II. IN CASE OF HOMOGENOUS 3D BULK STRUCTIRE

The calculated device is a simple n^+-n-n^+ structure (Fig. 1) in which MC window is a cubic structure of uniform doping with 100 nm size, and DD (drift-diffusion) region is settled outside of the window, where contacts are set in n^+ regions. In the simulation, particle state and potential are updated self-consistently, in which the number of particles assigned is the same as the actual number of electrons. The particle charge is assigned by the cloud-in-cell method. Acoustic and optical phonon scatterings are included and Coulomb scatterings are not included as the first stage of investigation. Details of our fullband simulator, HyDeLEOSMC, with coupled Monte Carlo-drift diffusion method are described elsewhere [6]. A snapshot of the calculated potential distribution is shown in Fig. 2.

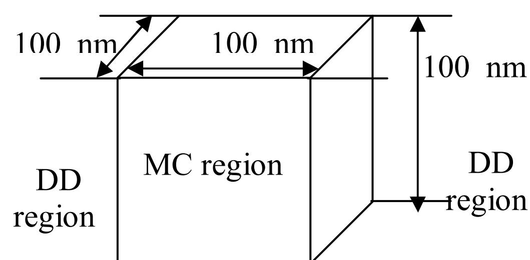

Figure 1. Simulated device structure, in which MC window is a cubic structure of uniform doping density. And its contacts are set in DD regions.

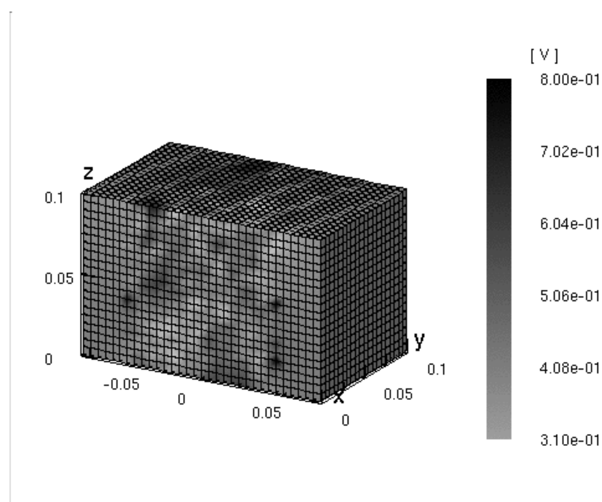

Figure 2. A snapshot of the calculated potential distribution (n = Nd = 10^{19} cm^{-3} as an example).

The amplitude of the potential fluctuation at each mesh is calculated and averaged over the values inside MC window where the boundary effect is negligible. In Fig. 3, calculated results are shown and compared with theoretical results by Fischetti et al. [2]. We employed 5 nm mesh spacing due to the recommended mesh spacing $\Delta x \approx n^{-1/3}$ in Ref. [2]. The results are comparable and between semi-classical and quantum-mechanical results. In Fig. 3 the amplitude of 2.5 nm mesh spacing is shown in comparison. As we found finer mesh

tended to cause instability in coupling continuity equation in DD region, we added error bars in the figure. The results are larger than those of 5 nm, due to '1/r' dependence formed by a point charge of an electron, so mesh spacing is subject to be carefully investigated.

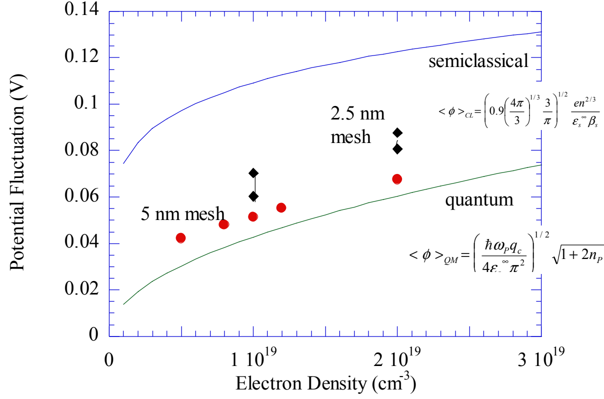

Figure 3. The root mean square amplitude of potential fluctuation (standard deviation) in thermal-equilibrium (T = 300 K). The symbols are the result of present simulation using 5 and 2.5 nm mesh spacings. The lines are the results of quantum-mechanical and semi-classical theoretical equations by Fischetti et al. (Eq. (35) and Eq. (41) or Fig. 2 of Ref. [2], shown in this figure).

Also the power spectral densities are shown in Fig. 4, which are derived from the Fourier series of the auto-correlation functions of potential fluctuation. The values are averaged over the values inside MC region. Clear peak is observed in Fig. 4.

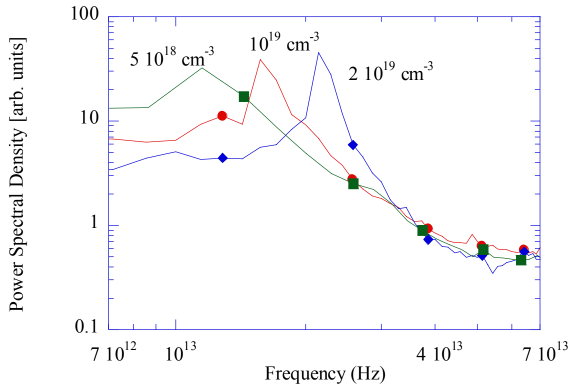

Figure 4. Power spectral densities of potential fluctuation with three cases of carrier concentration.

The peak frequencies in Fig. 4 are extracted and plotted as a function of carrier density in Fig. 5. These values were found to be in a good agreement with the theoretical plasma frequency. In these calculations, Poisson equation is updated at every 1 fs which is sufficiently smaller than inverse of plasma frequency.

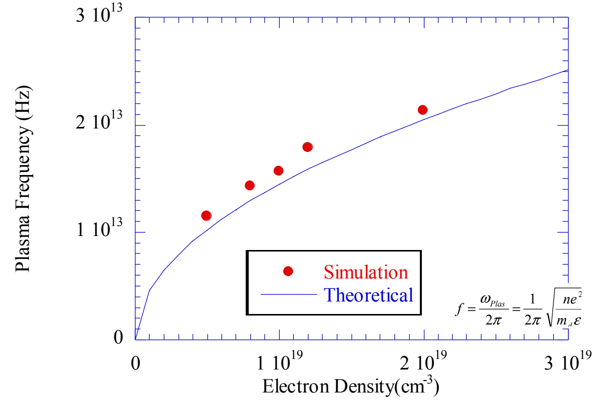

Figure 5. Extracted frequencies derived from the peaks of power spectral densities of potential fluctuation in Fig. 4 and the theoretical plasma frequencies.

In Fig.5, the slight deviation of frequency is observed. One of the reasons is thought to be inclusion of scatterings which was pointed out in Ref. [4]. So we calculated power spectral density with and without scattering as shown in Fig. 6 and confirms the results of Ref. [4]. The simulation without scattering is found to be unstable so, results of low temperature (77K) and high density (3 10^{19}cm^{-3}) is shown in the figure.

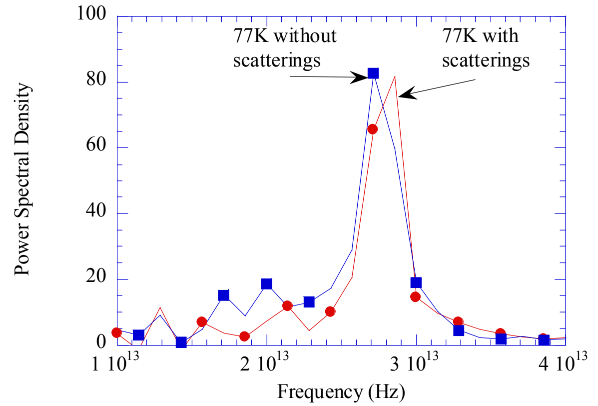

Figure 6. Power spectral densities of potential fluctuation with and without scatterings at 3 10^{19} cm^{-3}. Poisson equation is updated at every 0.5 fs.

In Fig. 7, temperature dependency of autocorrelation function is shown. Normalized autocorrelation function is defined as,

$$C_i(\tau) = \int_{t=t_0}^{t=t_{\max}-\tau} (\psi_i(t) - \bar{\psi}_i)(\psi_i(t+\tau) - \bar{\psi}_i)dt \Big/ \int_{t=t_0}^{t=t_{\max}-\tau} (\psi_i(t) - \bar{\psi}_i)^2 dt$$

where, t_0 is the initial integration time and t_{max} is the time when the simulation is ended and i denotes index of the mesh point, and, $\psi(t)$ is potential and $\bar{\psi}$ is time average of $\psi(t)$. The spatial average $C(\tau) = \overline{C_i(\tau)}$ for mesh points, where the boundary effect

is negligible, is shown in the figure. Though the calculated periodicity is not so changed by temperature, the correlations become less clearly with increase of temperature. As the main target in this paper was the understanding of the potential fluctuation in the channel where impurity scattering thought to be less dominant, the impurity scattering is not included in these calculations, thus these tendencies are mainly due to the increase of phonon scatterings with temperature.

In Fig. 7, the result with impurity scattering (I. S.) is denoted a dashed line. With impurity scattering, bulk mobility is known to be 1 order smaller than low doped silicon at 300K. The frequency of autocorrelation function with I. S. is slight larger than that without I. S., but very noisy as shown in Fig. 7, and its power spectral density, which will be shown elsewhere, was also too noisy though its peak for plasmon was observed.

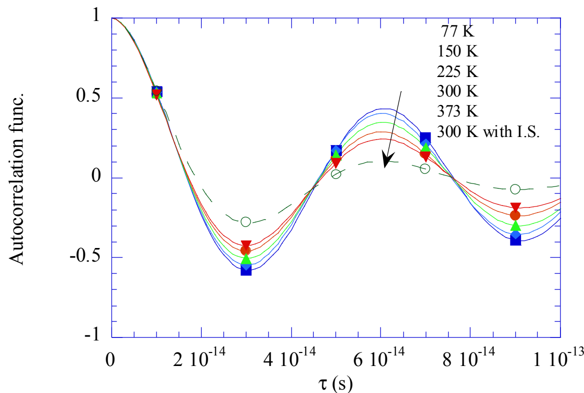

Figure 7. Temperature dependency of autocorrelation function of potential fluctuation at n = Nd = 10^{19} cm^{-3}.Solid lines are with phonon scatterings from 77K to 373K and dashed line (300K with I. S.) denotes with phonon and impurity scatterings at 300K.

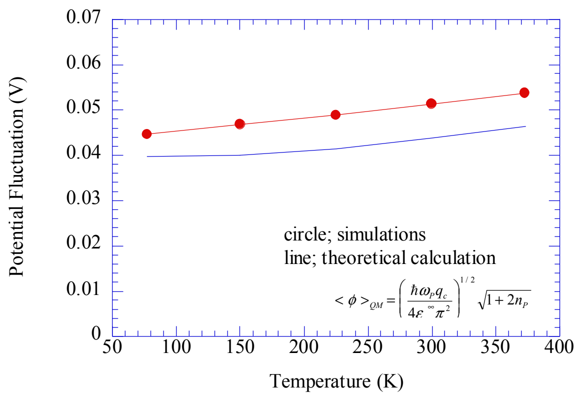

Figure 8. Temperature dependence of potential fluctuation compared with simulated results and theoretical results (Eq. (41) of Ref. [2]) for n = 10^{19} cm^{-3}.

Also temperature dependences of potential fluctuation are compared with simulated results and theoretical results are shown in Fig. 8. The calculated results are also larger but indicate the same temperature dependence compared with theoretical results. With impurity scatterings the strength of potential fluctuation decreased near to the theoretical results, which are under investigation and will be shown elsewhere, so the effect of scattering was found to be rather small.

III. IN CASE OF 3D BULK STRUCTURE

Next example is a fullband Monte Carlo simulation of a 3D MOSFET reported elsewhere [5] in which the number of particles assigned is the same as the actual number of electrons. The simulated structure and its potential distribution are shown in Fig. 9.

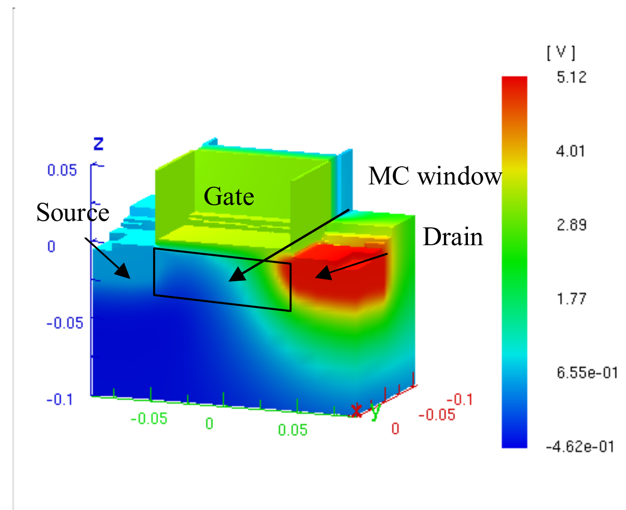

Figure 9. The calculated potential distribution of a 3D MOSFET (L_G/W_G = 90/110 nm, V_D/V_G = 4.5/2.5 V).

The distribution of the potential fluctuation along the direction perpendicular to the interface is shown in Fig. 10. As the mesh spacing is subject to further investigation because the recommended mesh spacing in Ref. [2] is hard to be employed in non-uniformity system, somewhat ‘typical’ non-uniform meshing is employed in this study. Poisson equation is updated at every 0.5 fs. Though the inversion carrier is located only near the interface, the potential fluctuation extends through the depletion region where any carriers are scarcely existed. The potential fluctuation is largest at near the interface of source side as carrier density is largest (about 10^{20} cm^{-3}) in the source side. On the other hand, potential fluctuation extended most widely as the extension of inversion carrier in the drain side, where the peak electron density was about 10^{18} cm^{-3}. So the amplitude of the potential fluctuation in the drain side is stronger than the expected value driven from the results of Fig. 3. This deviation is thought to be due to ‘hot’ and non-equilibrium electron-energy distribution. The temperature dependency of the theoretical model indicates the screening is weakened, and the number of plasmon is increased. In the simulation, carriers in the source and drain layers, where the potential fluctuation is thought to be strong, are treated by DD model in respect of the computational burden, as we were concentrated on the potential fluctuation in the non-equilibrium region in the channel.

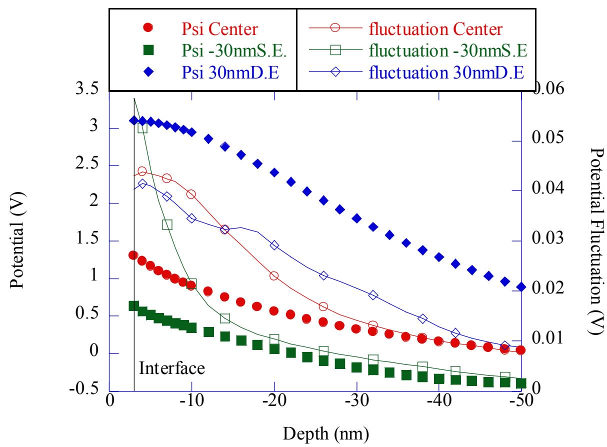

Figure 10. The distributions of averaged potentials and their potential fluctuations during simulation at $V_D = 4.5$ V, $V_G = 2.5$ V. The cross section along the depth direction the center, source side (-30 nm) and drain side (+30 nm) of the gate are shown.

In Fig. 11, distribution of potential (dots) and potential fluctuation (lines) along the surface for Vg = 2.5/3.5/4.5 V at (a) Vd = 0.1V and (b) Vd = 4.5 V is shown. The strength of potential fluctuation increases with gate voltage but same order with different drain voltage, this is correspondent to the weak temperature dependence of potential fluctuation shown in Fig. 7.

Power spectral density of potential fluctuation at the points corresponding to the surface points were too noisy though some peaks were observed in the neighbor of 10^{13} Hz, probably due to spaciously non-uniform carrier density. If sub-band system is considered, plasma frequency should be replaced by the surface plasma frequency, which has dispersion on wave-vector q [7].

So we should further investigate the effect of the potential fluctuation on the carrier mobility and carrier energy distribution especially in non-equilibrium bias condition. 3D Monte Carlo simulation is important tool to understand the potential fluctuation in realistic device operations.

IV. Conclusion

In this study, the potential fluctuation is investigated. In the uniform 3D structure, the amplitude of potential fluctuation and driven plasma frequency are evaluated and shown to be in good agreements with theoretical results. In 3D MOSFET, the potential fluctuation extends towards the depletion layer and deviation of the amplitude from theoretical value is observed and ascribed to hot electron energy distribution, so the conventional plasmon scattering model should be modified in non-uniform and non-equilibrium carrier distribution.

Acknowledgment

The authors would thank to Dr. N. Mori at Osaka University for discussion and suggestion about 2D plasmon.

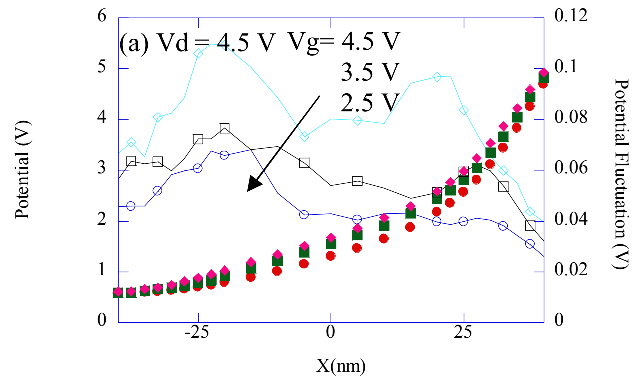

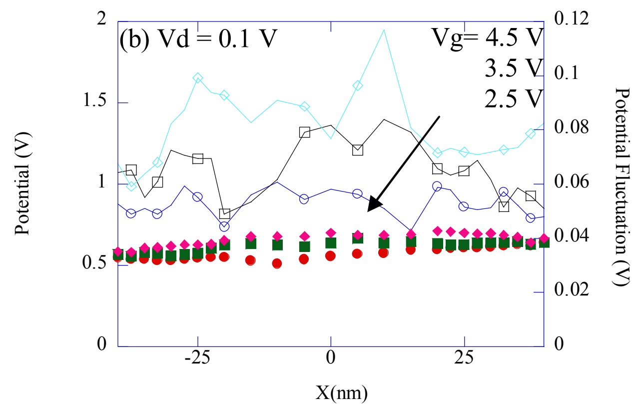

Figure 11. Distribution of potential (dots) and potential fluctuation (lines) along the surface for Vg = 2.5/3.5/4.5 V at (a) Vd = 0.1 V and (b) Vd = 4.5 V. Where gate edge of the source side is X = -45 nm and of the drain side is X = +45 nm.

References

[1] M. V. Fischetti and S. E. Laux, “Monte Carlo Analysis of Electron Transport in Small Semiconductor Devices Including Band-Structure and Space-Charge Effects,” Phys. Rev. B, vol. 38, no. 14, pp. 9721-9745, November 1988.

[2] M. V. Fischetti and S. E. Laux, “Long-Range Coulomb Interactions in Small Silicon Devices. Part I: Performance and Reliability,” J. Appl. Phys., vol. 89, no. 2, pp. 1205-1231, January 2001.

[3] H. Tsuchiya, A. Oda, M. Ogawa, and T. Miyoshi, “Quantum-Corrected Monte Carlo and Molecular Dynamics Simulation on Electron-Density-Dependent Velocity Saturation in Silicon Metal-Oxide-Semiconductor Field-Effect Transistors,” Jpn. J. Appl. Phys., vol. 44, no. 11, pp. 7820-7826, November 2005.

[4] T. Uechi, T. Fukui, and N. Sano “3D Monte Carlo simulation including full Coulomb interaction under high electron concentration regimes,” physica status solidi (c) vol. 5, no1, pp. 102-106, October 2007.

[5] Y. Ohkura and C. Suzuki, “Monte Carlo simulation of 3D nonvolatile memory”, SISPAD 2006, p. 279-282.

[6] Y. Ohkura, C. Suzuki, T. Enda, H. Takashino, H. Ishikawa, T. Kojima and T. Wada, “A 3-dimensional particle device simulator; HyDeLEOSMC and its application to a FinFET,” SISPAD 2005, pp. 287-290.

[7] T. Ando, B. Fowler and F. Stern, “Electronic properties of 2D systems,” Reviews of Modern Physics, vol. 54, pp.438-672, April 1982.